Macroscopic $1/f$ Behavior of Fractal Signals Generated by Additive Substitution

Tatiana Alieva and André Barbé, *Member, IEEE*

***Abstract*—We analyze the structure of the discrete Fourier transform of a particular class of self-similar discrete signals which are iteratively generated by an additive substitution procedure, starting from a finite generator sequence. The amplitude spectra of such signals obtained from different generators have a similar form. The amplitude spectrum contains several affine branches, the number of which depends on the iteration level, on the size of the generator, and on the spectrum's symmetry. It has a macroscopic $1/f$-characteristic.**

***Index Terms*—Deterministic fractal signals, discrete Fourier transform, $1/f$-behavior, scaling behavior.**

I. Introduction

Fractal signals describe a variety of processes arising in nature and sociology, for example, turbulence flow, fluid mixing, aggregation, data traffic on communication channels, music, etc. [11]. The typical property of such objects is that they are infinitely complex: a small portion of it is, in a certain way, similar to the original. In signal processing, ıe types of noise can be treated like fractal structures [8]. Moreover, fractal signals promise to be important for communication applications, because they transmit information that can be recovered at different scales [5], [10], [11].

Fractal structures are frequently associated with cascade processes and their models are generated through iterative procedures [9], [4]. Real-world fractal structures usually exhibit their self-affine properties only for a certain number of scales and are described in the model by a finite number of iterations n. In this correspondence we consider discrete signals, denoted by a row vector $\boldsymbol{f}_n$, constructed from the generator vector $\boldsymbol{f}_1$ of size M

$$\boldsymbol{f}_1 = [f_1(0), f_1(1), \ldots, f_1(m), \ldots, f_1(M-1)] \tag{1}$$

with $f_1(m) \in \mathbb{C}$ (the field of complex numbers), through the following additive iteration:

$$\boldsymbol{f}_n = \begin{bmatrix} [\boldsymbol{f}_{n-1}]^t + f_1(0) \\ [\boldsymbol{f}_{n-1}]^t + f_1(1) \\ \cdots \\ [\boldsymbol{f}_{n-1}]^t + f_1(M-1) \end{bmatrix}^t \tag{2}$$

($\boldsymbol{t}$ denotes transposition, $[\boldsymbol{f}_{n-1}]^t + a$ denotes that a is added to each element of $[\boldsymbol{f}_{n-1}]^t$).

This iteration scheme is the one-dimensional case, and extension in $\mathbb{C}$, of a particular class of integer fractal matrices that was introduced in [1] and further investigated in [2], [3]. We will here investigate the specific features of the Fourier amplitude spectrum of such signals $\boldsymbol{f}_n$.

The signal of level n

$$\boldsymbol{f}_n = [f_n(0), f_n(1), \ldots, f_n(m), \ldots, f_n(M^n-1)]$$

has M^n elements. Its elements can be written as

$$f_n(k + M^{n-1}m) = f_1(m) + f_{n-1}(k) \tag{3}$$

where $k = 0, \ldots, M^{n-1}-1$ and $m = 0, \ldots, M-1$. In what follows, the integer set $\{0, 1, \ldots, z-1\}$ will be denoted by $[z]$.

Iterating (3), we derive that jth element of sequence $\boldsymbol{f}_n$ can be represented in the form

$$f_n(j) = \sum_{s=0}^{n-1} f_1(m_s) \tag{4}$$

where

$$j = m_0 + m_1 M + \cdots + m_l M^l + \cdots + m_{n-1}M^{n-1} \in [M^n] \tag{5}$$

and $m_s \in [M]$ $(s = 0, 1, \ldots, n-1)$. This also means that the string $m_{n-1}m_{n-2}\ldots m_1 m_0$ is the n-digit base-M representation of j (possibly with leading 0's). Splitting the sum (5) into

$$j = \underbrace{m_0 + m_1 M + \cdots + m_{l-1}M^{l-1}}_{k \in [M^l]} + M^l \underbrace{(m_l + m_{l+1}M + \cdots + m_{n-1}M^{n-l-1})}_{q \in [M^{n-l}]} \tag{6}$$

it is easy to see that, for al $l = 1, \ldots, n$, $k \in [M^l]$, $q \in [M^{n-l}]$

$$f_n(k + M^l q) = f_l(k) + f_{n-l}(q). \tag{7}$$

Observe that from (3), it follows that the sequence of the first M^{n-k} elements of $\boldsymbol{f}_n$ equals $\boldsymbol{f}_{n-k}$ augmented with $kf_1(0)$. Formally

$$f_n(r) = f_{n-k}(r) + kf_1(0), \qquad r \in [M^{n-k}]. \tag{8}$$

As a consequence, when the first element of the generator $[f_1(0)]$ equals 0, $\boldsymbol{f}_n$ forms the leading sequence of $\boldsymbol{f}_m$ whenever $m \geq n$.

II. Self-Affinity Aspects of $\boldsymbol{f}_n$.

Self-Affinity Under Decimation

Let l and k be fixed in (7). The (M^l, k)-decimation of $\boldsymbol{f}_n$, denoted by $D_{M^l,k}(\boldsymbol{f}_n)$, is the sequence consisting of the M^{l-n} elements

Manuscript received November 16, 1998; revised February 28, 2000. This work was supported in part under a Concerted Action Project of the Flemish Community (GOA-MIPS), and by the Belgian Program on Interuniversity Attraction Poles, Prime Minister's Office for Science, Technology and Culture (IUAP P4-02). The material in this correspondence was presented in part at the International Conference on Accoustics, Speech, and Signal Processing (ICASSP'99), Phoenix, AZ, May 15–19, 1999.

The authors are with the Department of Electrical Engineering, Katholieke Universiteit Leuven, B-3001 Leuven, Belgium (e-mail: Andre.Barbe@esat.kuleuven.ac.be).

Communicated by T. E. Fuja, Associate Editor At Large.
Publisher Item Identifier S 0018-9448(00)07013-9.

0018–9448/00$10.00 © 2000 IEEE

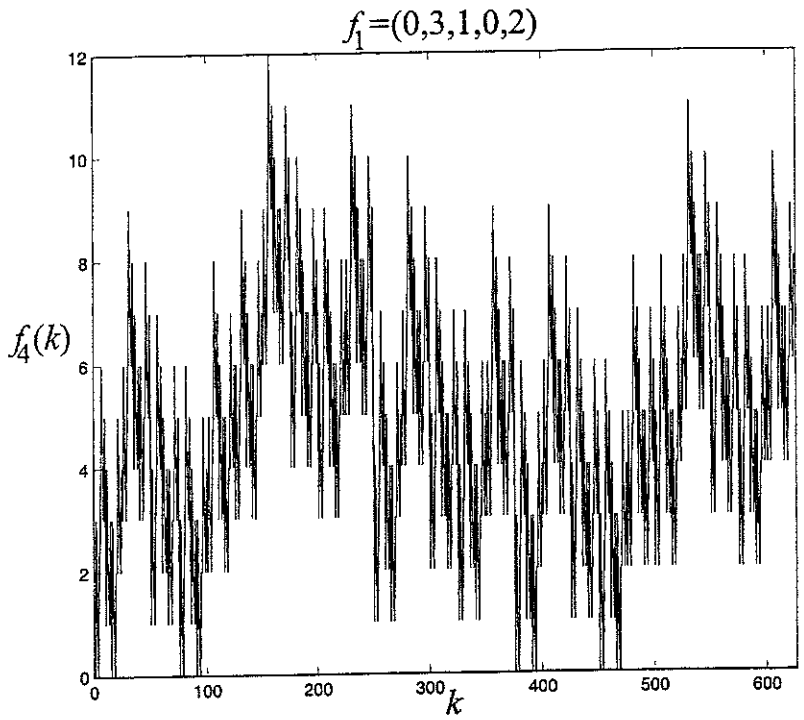


Fig. 1. Graphical representation of the signal $\boldsymbol{f}_4$ obtained from the generator $\boldsymbol{f}_1 = [0, 3, 1, 0, 2]$ (linear interpolation between the $f_4(k)$-values).

$f_n(k + M^l q), q \in [M^{n-l}]$. Equation (7) then shows that this decimation sequence is affine to the sequence $\boldsymbol{f}_{n-l}$ (through the addition of the fixed element $f_l(k)$ to all elements in $\boldsymbol{f}_{n-l}$)

$$D_{M^l,k}(\boldsymbol{f}_n) = \boldsymbol{f}_{n-l} + f_l(k).$$

Collage Property: Now fix l and q in (7), and let k range over $[M^l]$, i.e., consider the subsequence $\boldsymbol{f}_{n,l;q} = (f_n(k))_{k \in qM^l + [M^l]}$. It consists of M^l consecutive elements of $\boldsymbol{f}_n$, starting at qM^l. Then it follows that

$$\boldsymbol{f}_{n,l;q} = \boldsymbol{f}_l + f_{n-l}(q) \tag{9}$$

i.e., $\boldsymbol{f}_{n,l;q}$ is affine to $\boldsymbol{f}_l$. The whole signal $\boldsymbol{f}_n$ consists of M^{l-n} concatenated copies of $\boldsymbol{f}_l$ which are placed at the points $qM^l, q \in [M^{n-l}]$, where the copy placed at qM^l is augmented by $f_{n-l}(q)$.

Self-Affinity Under Coarse Graining: Consider the average s_n of all elements in $\boldsymbol{f}_n$, i.e.,

$$s_n = \frac{1}{M^n} \sum_{j=0}^{M^n-1} f_n(j)$$

and let

$$s_{n,l;q} = \frac{1}{M^l} \sum_{j=0}^{M^l-1} f_n(qM^l + j)$$

be the average of all elements in $\boldsymbol{f}_{n,l;q}$. Then it follows from (9) that $s_{n,l;q} = f_{n-l}(q) + s_l$. As a consequence, the sequence of the averages of the subsequences $\boldsymbol{f}_{n,l;q}$ is affine to $\boldsymbol{f}_{n-l}$

$$(s_{n,l;q})_{q \in [M^l]} = \boldsymbol{f}_{n-l} + s_l.$$

This uncovers a self-similarity of $\boldsymbol{f}_n$ under its coarse graining obtained by averaging the subsequences $\boldsymbol{f}_{n,l;q}$. As

$$s_n = \frac{1}{M^{n-l}} \sum_{q=0}^{M^{n-l}-1} s_{n,l;q}$$

$$= \frac{1}{M^{n-l}} \sum_{q=0}^{M^{n-l}-1} [f_{n-l}(q) + s_l] = s_{n-l} + s_l \tag{10}$$

also yielding $s_n = ns_1$, it follows that $s_1 = 0$ implies that $s_n = 0$ for all n. Then the average value of all $\boldsymbol{f}_n$ equals 0, and $(s_{n,l;q})_{q \in [M^l]} = \boldsymbol{f}_{n-l}$.

Some of the above-mentioned self-similarities can easily be retraced in Fig. 1, which shows a graphical representation of the fourth-generation sequence $\boldsymbol{f}_4$ constructed from the generator $\boldsymbol{f}_1 = [0, 3, 1, 0, 2]$.

Self-Affinity of the Partial-Sum Sequence: Define

$$a_n(m) = \frac{1}{m} \sum_{i=0}^{m-1} f_n(i)$$

the average of the first m elements of $\boldsymbol{f}_n$. Then

$$a_n(kM^u) = a_n(k) + u[s_1 - f_1(0)] \tag{11}$$

$$a_{n+k}(m) = a_n(m) + kf_1(0). \tag{12}$$

Indeed,

$$a_n(kM^n) = \frac{1}{kM^{n-1}} \sum_{q=0}^{kM^{n-1}-1} \frac{1}{M} \sum_{j=0}^{M-1} f_n(qM + j)$$

$$= \frac{1}{kM^{n-1}} \sum_{q=0}^{kM^{n-1}-1} s_{n,1;q}$$

$$= \frac{1}{kM^{n-1}} \sum_{q=0}^{kM^{n-1}-1} [f_{n-1}(q) + s_1]$$

$$= s_1 + \frac{1}{kM^{n-1}} \sum_{q=0}^{kM^{n-1}-1} f_{n-1}(q). \tag{13}$$

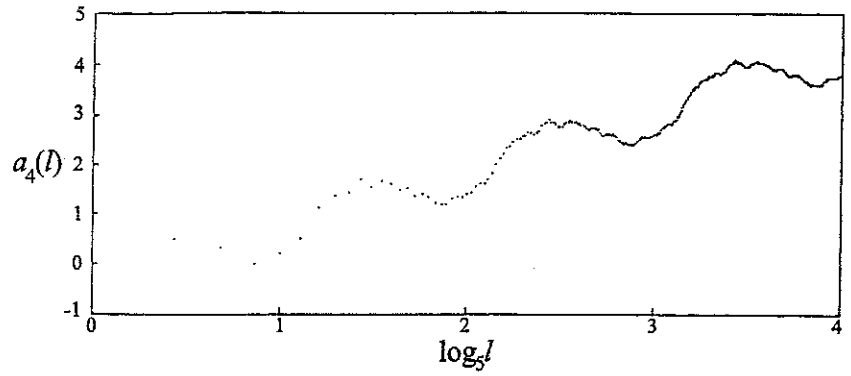


Fig. 2. The partial sum sequence $(a_4(l))_{l=1,\ldots,5^4-1}$ of the signal presented in Fig. 1 ($\boldsymbol{f}_1 = [0, 3, 1, 0, 2]$). Observe the "periodic" behavior superposed on a linear drift in this graph.

Now, use (8) with $k = 1$ to transform (13) into

$$a_n(kM^u) = s_1 + \frac{1}{kM^{u-1}} \sum_{q=0}^{kM^{u-1}-1} [f_n(q) - f_1(0)]$$
$$= a_n(kM^{u-1}) + [s_1 - f_1(0)].$$

Iterate this $u-1$ times to obtain (11). Equation (12) is obtained from using (8) in the definition of $a_{n+k}(m)$.

From (11), it follows that when we consider the graph of $a_n(\log_M m)$, we find *periodic* behavior superposed on a *linear drift*

$$a_n(u + \log_M k) = a_n(\log_M k) + u[s_1 - f_1(0)].$$

This is illustrated in Fig. 2. Notice that the linear drift disappears when $f_1(0) = s_1$, i.e., when the first element of the generator equals the generator's average. In that case, the sequence $(a_n(k))_{k=1,2,\ldots,M^n}$ for $n \to \infty$ is completely invariant under M^u-decimation: $a_n(kM^u) = a_n(k)$ (for any integers k, $u \geq 0$).

III. Discrete Fourier Transform of $\boldsymbol{f}_n$.

The discrete Fourier transform (DFT) of a sequence $\boldsymbol{f}_n = (f_n(0), f_n(2), \ldots, f_n(M^n - 1))$ is given by [6]

$$F_n(l) = \frac{1}{M^n} \sum_{k=0}^{M^n-1} f_n(k) \exp\left(-\frac{i2\pi lk}{M^n}\right) \tag{14a}$$

$$= \frac{1}{M^n} \sum_{m=0}^{M-1} \sum_{k=0}^{M^{n-1}-1} f(k + M^{n-1}m) \cdot \exp\left(-\frac{i2\pi l(k + M^{n-1}m)}{M^n}\right) \tag{14b}$$

where l is an integer. It is well known that this DFT is periodic with period M^n

$$F_n(l + M^n k) = F_n(l). \tag{15}$$

Therefore, we will investigate the structure of $\boldsymbol{F}_n$ in the region $l \in [M^n]$.

Substituting (3) in (14b) we get

$$F_n(l) = \frac{1}{M^n} \sum_{k=0}^{M^{n-1}-1} \sum_{m=0}^{M-1} (f_{n-1}(k) + f_1(m)) \cdot \exp\left(-\frac{i2\pi l}{M^n}(k + mM^{n-1})\right)$$
$$= \frac{1}{M^n} \sum_{k=0}^{M^{n-1}-1} f_{n-1}(k) \exp\left(-\frac{i2\pi lk}{M^n}\right) \sum_{m=0}^{M-1} \exp\left(-\frac{i2\pi lm}{M}\right)$$
$$+ \frac{1}{M^n} \sum_{m=0}^{M-1} f_1(m) \exp\left(-\frac{i2\pi lm}{M}\right) \sum_{k=0}^{M^{n-1}-1} \exp\left(-\frac{i2\pi lk}{M^n}\right). \tag{16}$$

We will derive some relationships between the $\boldsymbol{F}_n$ for different iteration steps n, taking into account that

$$\sum_{m=0}^{M-1} \exp\left(-\frac{i2\pi lm}{M}\right) = \begin{cases} 0, & \text{if } l \neq pM, \text{ where } p \text{ is an integer} \\ M, & \text{if } l = pM, \end{cases} \tag{17}$$

and

$$\sum_{k=0}^{M^{n-1}-1} \exp\left(-\frac{i2\pi lk}{M^n}\right) = \begin{cases} 0, & \text{if } l = pM, \ p \text{ is an integer}, \ p \neq 0 \\ M^{n-1}, & \text{if } l = 0 \\ \frac{\exp(-i\pi l/M)}{\exp(-i\pi l/M^n)} \frac{\sin(\pi l/M)}{\sin(\pi l/M^n)}, & \text{if } l \neq pM, \ p \text{ is an integer.} \end{cases} \tag{18}$$

First of all, it is easy to see from (3) and (14) that $F_n(0)$, which equals the average value of the sequence, satisfies

$$F_n(0) = \frac{1}{M^n} \sum_{k=0}^{M^n-1} f_n(k)$$
$$= \frac{1}{M^n} \sum_{k=0}^{M^{n-1}-1} \sum_{m=0}^{M-1} (f_{n-1}(k) + f_1(m))$$
$$= F_{n-1}(0) + F_1(0) \tag{19}$$

which, after n iterations, yields

$$F_n(0) = nF_1(0). \tag{20}$$

In what follows, $F_n(0)$ will be of no importance: it can always be brought to zero without affecting the rest of the spectrum by substracting $F_n(0)$ from all $f_n(k)$ (for sequences obtained from a generator with average value 0, $F_n(0)$ is automatically 0). Using (16) and (18), one finds that $\boldsymbol{F}_n$ restricted to the M-decimated point set $\{pM | p \in [M^{n-1}]\}$ corresponds to the DFT of $\boldsymbol{f}_{n-1}$

$$F_n(pM) = \frac{1}{M^{n-1}} \sum_{k=1}^{M^{n-1}-1} f_{n-1}(k) \exp\left(-\frac{i2\pi kp}{M^{n-1}}\right) = F_{n-1}(p). \tag{21}$$

Iterating (21) then yields for $p \in [M^{n-q}]$

$$F_n(pM^q) = F_{n-q}(p). \tag{22}$$

As follows from (16) and (18), the DFT of $\boldsymbol{f}_n$ at points $l \neq pM$ can be written as

$$F_n(l)|_{l \neq pM} = \frac{1}{M^{n-1}} \frac{\exp(-i\pi l/M)}{\exp(-i\pi l/M^n)} \frac{\sin(\pi l/M)}{\sin(\pi l/M^n)} F_1(l). \tag{23}$$

We will now investigate the implications of (21) and (23) on the structure of the graph of $\boldsymbol{F}_n$. In what follows, if A is some set of numbers and α is a number, αA will denote the set obtained by multiplying all elements in A by α. $|A|$ denotes the cardinality of A.

Let $\mathcal{D}_n \stackrel{\text{def}}{=} \{1, 2, \ldots, M^n - 1\}$denote the domain of interest for $F_n(l)$, and let

$$\mathcal{B}_q^n \stackrel{\text{def}}{=} \mathcal{D}_n \cap \{kM^{n-q} | k \in \mathbb{N}\}$$

be the set of multiples of M^{n-q} in $\mathcal{D}_n$. It follows that

$$\emptyset = \mathcal{B}_0^n \subset \mathcal{B}_1^n \subset \mathcal{B}_2^n \subset \mathcal{B}_3^n \subset \cdots \mathcal{B}_n^n = \mathcal{D}_n.$$

Then the set

$$\left\{\mathcal{A}_q^n \stackrel{\text{def}}{=} \mathcal{B}_q^n \backslash \mathcal{B}_{q-1}^n | q = 1, \ldots, n\right\}$$

forms a *hierarchical partition* of $\mathcal{D}_n$. $\mathcal{A}_q^n$ is the set of those elements in $\mathcal{D}_n$ that are multiples of M^{n-q} but not of M^{n-q+1}. It is an elementary exercise to show that this partition can be obtained in a more practical way by the recursion

$$\mathcal{A}_q^n = \mathcal{D}_n \cap M\mathcal{A}_{q+1}^n, \qquad q = n-1, n-2, \ldots, 1 \tag{24}$$

starting with $\mathcal{A}_n^n$, the set of elements of $\mathcal{D}_n$ which are *not* a multiple of M. Equation (24) also leads to $\mathcal{A}_q^n = \mathcal{D}_n \cap M^{n-q}\mathcal{A}_n^n$. It also holds that $|\mathcal{A}_q^n| = M^{q-1}(M-1) = M|\mathcal{A}_{q-1}^n|$.

For example, with $M = 5$, $n = 4$, we have

$$\begin{aligned}
\mathcal{D}_4 &= \{1, 2, 3, 4, 5, \ldots, 623, 624\} \\
\mathcal{A}_4^4 &= \{1, \underline{2}, 3, 4, , 6, \underline{7}, 8, 9, , 11, \underline{12}, 13, 14, , \\
&\qquad 16 \ldots 619, , 621, \underline{622}, 623, 624\} \\
\mathcal{A}_3^4 &= \{\underline{5}, 10, 15, 20, , \underline{30}, 35, 40, 45, , \underline{55} \ldots 595, , \\
&\qquad \underline{605}, 610, 615, 620\} \\
\mathcal{A}_2^4 &= \{25, 50, \underline{75}, 100, , 150, 175, \underline{200}, 225, , \\
&\qquad 275 \ldots 475, , 525, 550, \underline{575}, 600\} \\
\mathcal{A}_1^4 &= \{125, 250, 375, \underline{500}\}.
\end{aligned}$$

(The meaning of the underlined numbers will be explained later).

When moving from $\boldsymbol{f}_{n-1}$ to $\boldsymbol{f}_n$, the corresponding hierarchical partition associated with $\boldsymbol{F}_n$ can be constructed from the hierarchical partition associated with $\boldsymbol{F}_{n-1}$, using the relationship

$$\mathcal{A}_q^n = M\mathcal{A}_q^{(n-1)}, \qquad \text{for } q = 1, \ldots, n-1 \tag{25a}$$

$$\mathcal{A}_n^n = \mathcal{D}_n \backslash M\mathcal{D}_{n-1}. \tag{25b}$$

Equation (25b) implies $\mathcal{D}_n = \mathcal{A}_n^n \cup M\mathcal{D}_{n-1}$. From this last expression, and from (21) and (23), it then follows that

$$F_n(l) = F_{n-1}\left(\frac{l}{M}\right), \qquad \text{when } l \in M\mathcal{D}_{n-1} = \mathcal{B}_{n-1}^n \tag{26a}$$

$$F_n(l) = \frac{1}{M^{n-1}} \frac{\exp(-i\pi l/M)}{\exp(-i\pi l/M^n)} \frac{\sin(\pi l/M)}{\sin(\pi l/M^n)} F_1(l), \quad \text{when } l \in \mathcal{A}_n^n. \tag{26b}$$

Iterating (26) k times $(1 \leq k \leq n-1)$ yields

$$F_n(l) = F_{n-k}(l/M^k), \qquad \text{when } l \in \mathcal{B}_{n-k}^n \tag{27a}$$

$$\begin{aligned}
F_n(l) &= F_{n-r}(l/M^r) \\
&= \frac{1}{M^{n-r-1}} \frac{\exp(-i\pi l/M^{r+1})}{\exp(-i\pi l/M^n)} \frac{\sin(\pi l/M^{r+1})}{\sin(\pi l/M^n)} F_1(l/M^r), \\
&\qquad \text{when } l \in M^r\mathcal{A}_{n-r}^{n-r} \stackrel{(25a)}{=} \mathcal{A}_{n-r}^n, \; r < k.
\end{aligned} \tag{27b}$$

$\boldsymbol{F}_n$ as restricted to the domain $l \in \mathcal{A}_q^n$ will further be denoted by $\boldsymbol{F}_{n;\,q}$. It is then clear that $\boldsymbol{F}_n = \cup_{q=1}^n \boldsymbol{F}_{n;\,q}$. $F_{n;\,q}(l)$ represents a value only when $l \in \mathcal{A}_q^n$.

IV. Amplitude Spectrum of $\boldsymbol{f}_n$

Let us now consider the graph $\mathcal{G}(|\boldsymbol{F}_n|)$ of the amplitude spectrum $|F_n(l)|$, i.e., the point set $\{(l, |F_n(l)|) \,|\, l \in \mathcal{D}_n\}$ represented in the $(l, |F_n(l)|)$-coordinate plane.

As far as the amplitude spectrum is concerned, (27b) gives, for $q = 1, \ldots, n$

$$|F_{n;\,q}(l)| = \frac{1}{M^{q-1}} \left|\frac{\sin(\pi l/M^{n-q+1})}{\sin(\pi l/M^n)}\right| \left|F_1\left(\frac{l}{M^{n-q}}\right)\right|, \qquad \text{when } l \in \mathcal{A}_q^n. \tag{28}$$

Define

$$l_q \stackrel{\text{def}}{=} l/M^{n-q}.$$

Under the given condition $l \in \mathcal{A}_q^n$, l_q is an integer that is not a multiple of M (actually, l_q ranges over $\mathcal{A}_q^q$ when l ranges over $\mathcal{A}_q^n$), and we can write (28) as

$$|F_{n;\,q}(l)| = \frac{1}{M^{q-1}} |\sin(\pi l_q/M) F_1(l_q)| \, [\sin(\pi l/M^n)]^{-1}. \tag{29}$$

As both $|\sin(\pi l_q/M)|$ and $|F_1(l_q)|$ are M-periodic in l_q, we can write (29) also as

$$|F_{n;\,q}(l)| = M^{1-q} C(l_q \bmod M) [\sin(\pi l/M^n)]^{-1} \tag{30}$$

where

$$C(m) \stackrel{\text{def}}{=} |F_1(m) \sin(\pi m/M)|.$$

Observe that $m = l_q \bmod M$ in (30) can only take the values $1, 2, \ldots, M-1$ (not the value 0 because $l_q \bmod M \neq 0$ for $l \in \mathcal{A}_q^n$), and as a consequence, $C(m)$ has at most $M-1$ possible values in general. However, when the elements of the generator $\boldsymbol{f}_1$ are all real, $C(m)$ can take at most $\lfloor M/2 \rfloor$ values. Indeed, in this case, it holds that $|F_1(m)| = |F_1(M-m)|$, and as also

$$|\sin(\pi m/M)| = |\sin(\pi(M-m)/M)|$$

it follows that $C(m) = C(M-m)$.

The numbers $l \in \mathcal{A}_q^n$ for which $C(l_q \bmod M) = C(m)$ with m constant, are those elements of $\mathcal{A}_q^n$ for which $l/M^{n-q} \bmod M = m$, or for which $l = M^{n-q}(kM + m)$, $k \in \mathbb{N}$. Let us call this number set $\mathcal{A}_{q,\,m}^n$

$$\mathcal{A}_{q,\,m}^n = \mathcal{A}_q^n \cap \left\{mM^{n-q} + kM^{n-q+1} \,|\, k \in \mathbb{N}\right\}.$$

When the elements of $\mathcal{A}_q^n$ are listed in increasing order, $\mathcal{A}_{q,\,m}^n$ is obtained from the M-decimation of this list starting at the mth element. This is illustrated by referring to the previous $\mathcal{A}_q^4$ examples (for $M = 5$). $\mathcal{A}_{4,\,2}^4$, $\mathcal{A}_{3,\,1}^4$, $\mathcal{A}_{2,\,3}^4$, and $\mathcal{A}_{1,\,4}^4$ are given, respectively, by the underlined numbers in $\mathcal{A}_4^4$, $\mathcal{A}_3^4$, $\mathcal{A}_2^4$, and $\mathcal{A}_1^4$.

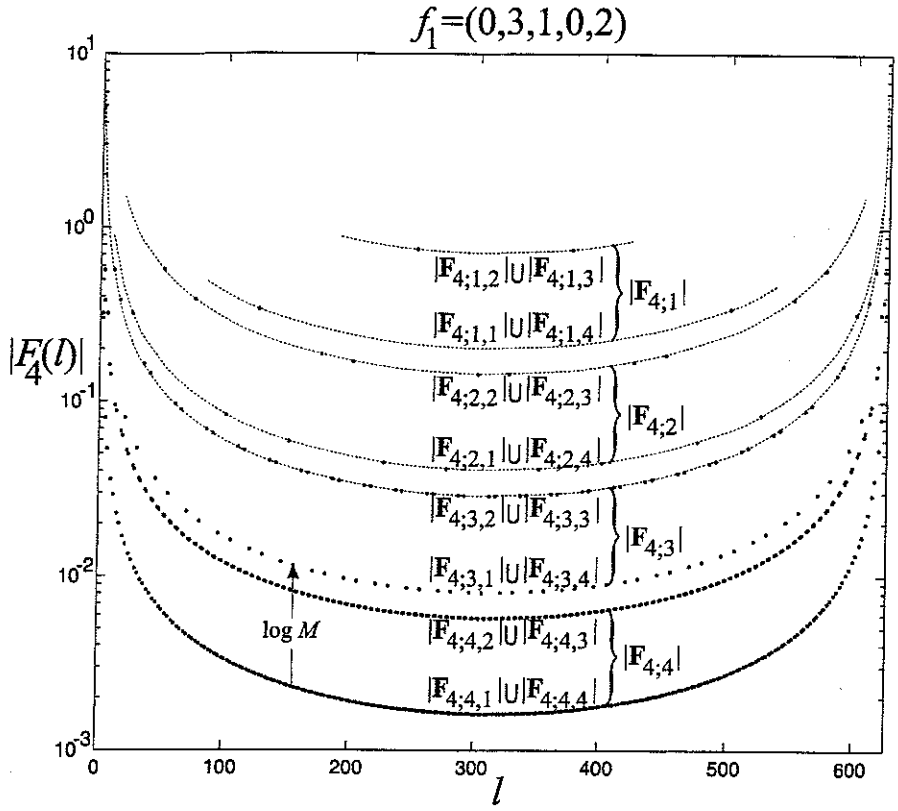


Fig. 3. The graph (big dots) $\mathcal{G}(\log|\boldsymbol{F}_4|) = \cup_{q=1}^{4}\mathcal{G}(\log|\boldsymbol{F}_{4;q}|) = \cup_{q=1}^{4}\cup_{m=1}^{4}\mathcal{G}(\log|\boldsymbol{F}_{4;q,m}|)$ for the signal $\boldsymbol{f}_4$ shown in Fig. 1, and generated from $\boldsymbol{f}_1 = [0, 3, 1, 0, 2](M = 5)$. $\boldsymbol{f}_1$ being real, there are $\lfloor M/2\rfloor \times n = \lfloor 5/2\rfloor \times 4 = 8$ branches (four groups of two branches). The subgraphs $\mathcal{G}(\log|\boldsymbol{F}_{4;q,1}|)$ and $\mathcal{G}(\log|\boldsymbol{F}_{4;q,4}|)$, q fixed, lie on the same branch; so do $\mathcal{G}(\log|\boldsymbol{F}_{4;q,2}|)$ and $\mathcal{G}(\log|\boldsymbol{F}_{4;q,3}|)$. The branches themselves are the graphs of the interpolation functions: $\mathcal{G}(\log|\boldsymbol{F}_{4;q,m}|^*) = \mathcal{G}[\log C(m)M^{1-q} - \log\sin(\pi l^*/M^4)]$ (thin dotted lines). $F_{4;q(,m)}(l)$ is defined only for $l \in \mathcal{A}^4_{q(,m)}$. The graphs of $|\boldsymbol{F}_j|$, $j < 4$ are present in this $|\boldsymbol{F}_4|$ graph as $\cup_{q=1}^{j}\mathcal{G}(|\boldsymbol{F}_4;\, q|)$, with the corresponding l values scaled down by the factor M^{4-j} (or, $|\boldsymbol{F}_j|$ is the M^{4-j}-decimation of $|\boldsymbol{F}_4|$).

It is elementary to show that for fixed n and q, the set $\{\mathcal{A}^n_{q,m}|m = 1, \ldots, M-1\}$ forms a partition of $\mathcal{A}^n_q$, and that none of the $\mathcal{A}^n_{q,m}$-sets is empty.

Denote by $\boldsymbol{F}_{n;q,m}$ the partial function obtained from $\boldsymbol{F}_n$ by restricting its domain to $\mathcal{A}^n_{q,m}$. Then (30) translates into

$$|F_{n;q,m}(l)| = M^{1-q}C(m)[\sin(\pi l/M^n)]^{-1}, \qquad m = 1, \ldots, M-1,\ q = 1, \ldots, n. \quad (31)$$

Define the "natural interpolation" $|\boldsymbol{F}_{n;q,m}|^*$ of $|\boldsymbol{F}_{n;q,m}|$ as the extension of (31) over the continuum-interval $[0, M^n]$, i.e.,

$$|F_{n;q,m}|^*(l^*) = M^{1-q}C(m)[\sin(\pi l^*/M^n)]^{-1}, \qquad l^* \in [0, M^n]. \quad (32)$$

Denote the graph of a function $\boldsymbol{F}$ by $\mathcal{G}(\boldsymbol{F})$ (i.e., the representation of $\mathcal{G}(\boldsymbol{F}) = \{(l, F(l))|l \in \operatorname{dom}\boldsymbol{F}\}$ as a point set in the $(l, F(l))$-plane). Then it is clear that

$$\mathcal{G}(|\boldsymbol{F}_{n;q}|) = \bigcup_{m=1}^{M-1}\mathcal{G}(|\boldsymbol{F}_{n;q,m}|) = \bigcup_{m=1}^{M-1}\mathcal{G}(|\boldsymbol{F}_{n;q,m}|^*)|_{\mathcal{A}^n_{q,m}} \quad (33)$$

meaning that the graph of $|\boldsymbol{F}_{n;q}|$ consists of points which are distributed over the graphs of $M-1$ interpolation functions $\mathcal{G}(|\boldsymbol{F}_{n;q,m}|^*)$ $(m = 1, \ldots, M-1)$. The graphs of these interpolation functions are magnitude-scaled versions of the graph of $[\sin(\pi l^*/M^n)]^{-1}$, the scaling factor being $M^{1-q}C(m)$. As $C(m)$ may generally take (at most) $(M-1)$ values ($\lfloor M/2\rfloor$ values when $\boldsymbol{f}_1$ is real), this means that the points of $\mathcal{G}(|\boldsymbol{F}_{n;q}|)$—for n, q fixed—are generally distributed over $(M-1)$ or $\lfloor M/2\rfloor$ branches which are all scaled versions of $\mathcal{G}([\sin(\pi l^*/M^n)]^{-1})$.

Keeping n fixed, but considering $\mathcal{G}(|\boldsymbol{F}_{n;q}|)$ and $\mathcal{G}(|\boldsymbol{F}_{n;q'}|)$ for $q \neq q'$, we see that the corresponding subgraphs $\mathcal{G}(|\boldsymbol{F}_{n;q,m}|)$ and $\mathcal{G}(|\boldsymbol{F}_{n;q',m}|)$ (m fixed) lie on the branches $\mathcal{G}(|\boldsymbol{F}^*_{n;q,m}|)$ and $\mathcal{G}(|\boldsymbol{F}^*_{n;q',m}|)$, respectively. The second branch is just a *magnitude-scaled* version of the first one, the scale factor is $M^{q-q'}$. This means that the $\mathcal{G}(|\boldsymbol{F}_{n;q'}|)$-parts of $\mathcal{G}(|\boldsymbol{F}_n|)$ lie on a similar set of branches as the $\mathcal{G}(|\boldsymbol{F}_{n;q}|)$-part, but magnitude-scaled by a factor $M^{q-q'}$. From this, and from the fact that

$$\mathcal{G}(|\boldsymbol{F}_n|) = \bigcup_{q=1}^{n}\mathcal{G}(|\boldsymbol{F}_{n;q}|) = \bigcup_{q=1}^{n}\bigcup_{m=1}^{M-1}[\mathcal{G}(|\boldsymbol{F}_{n;q,m}|^*)|_{\mathcal{A}^n_{q,m}}]$$

it follows that the points of $\mathcal{G}(|\boldsymbol{F}_n|)$ are distributed over (at most) $n \times D_M$ branches that are all magnitude-scaled versions of $\mathcal{G}([\sin(\pi l^*/Mn)]^{-1})$. $D_M = \lfloor M/2\rfloor$ when $\boldsymbol{f}_1$ is real, or $(M-1)$ otherwise. When considering $\mathcal{G}(\log|\boldsymbol{F}_n|)$, this scaling corresponds to a mere vertical shift: all $n \times D_M$ branches in this graph have the identical shape of $\mathcal{G}(-\log\sin(\pi l^*/M^n))$.

These properties concerning the structure of $\mathcal{G}(|\boldsymbol{F}_n|)$ are illustrated in two examples: the $(M = 5, n = 4)$ case with $\boldsymbol{f}_1 = [0, 3, 1, 0, 2]$ (Fig. 3); and the $(M = 3, n = 6)$ case with $\boldsymbol{f}_1 = [0, 3, 1]$ (Fig. 4). Recall that the DFT is periodic, and that the part with domain $[\lfloor\frac{M^n+1}{2}\rfloor, M^n - 1]$ also corresponds to the negative modes in the interval $[-M^n + \lfloor\frac{M^n+1}{2}\rfloor, -1]$.

Observe that for $|l|^* \ll M^n$, the interpolation function for all branches, as given by (32), behaves like $(|l|^*)^{-1}$. This can be clearly seen in Fig. 5, representing the graph $\{(\log(l), \log|F_n(l)|)|l \in \mathcal{D}_n\}$

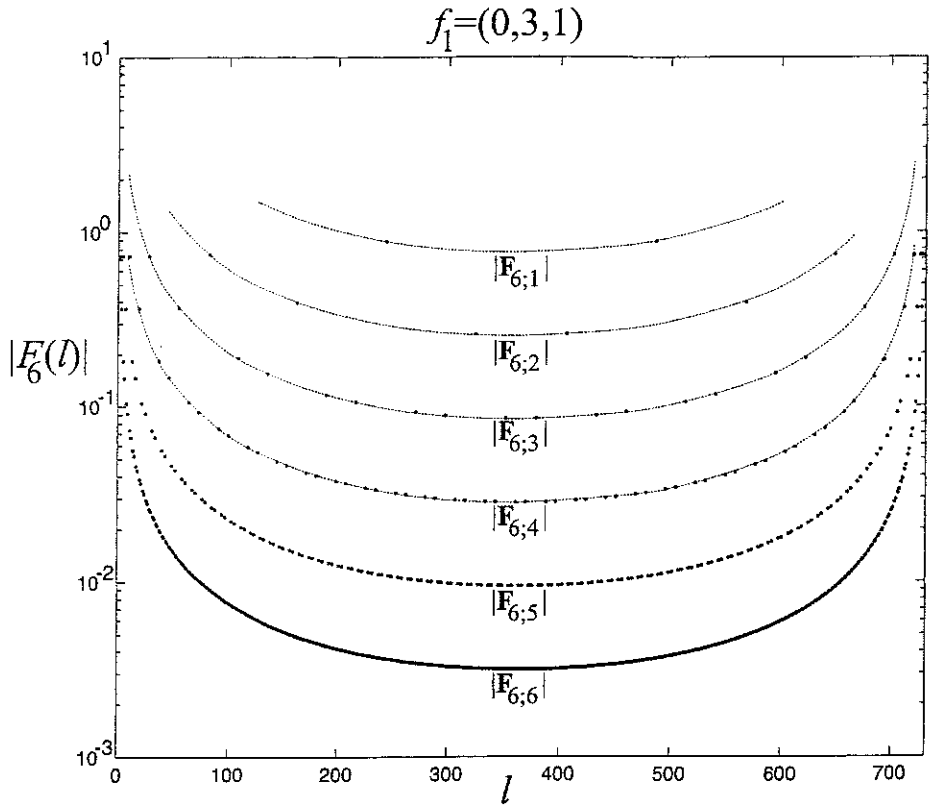


Fig. 4. The graph $(l, \log|F_6(l)|)$ of the amplitude spectrum of the signal $\boldsymbol{f}_6$ generated from the generator $\boldsymbol{f}_1 = [0, 3, 1]$ (size $M = 3$). $\boldsymbol{f}_1$ being real, there are $\lfloor M/2 \rfloor \times n = \lfloor 3/2 \rfloor \times 6 = 6$ branches. $|F_{6;q,1}|$ and $|F_{6;q,2}|$ lie on the same branch and form together $F_{6;q}$.

for a signal produced from a complex generator. It gives the whole amplitude spectrum a kind of macroscopic $1/|l|$ behavior consisting of $n \times D_M$ microscopic $1/|l|$ branches. Note that this $1/|l|$ behavior is independent of the size and values of the generator vector and of the generation level of the signal considered.

V. Concluding Remarks

We have introduced deterministic finite sequences $\boldsymbol{f}_n$ with particular self-similar features, grown from an generator sequence $\boldsymbol{f}_1$ with M elements. We have shown that the corresponding DFT-*amplitude* spectrum $|\boldsymbol{F}_n|$ consists of n groups of $(M-1)$ or $(\lfloor M/2 \rfloor)$ "branches" with approximate $1/f$ behavior. We suggest to qualify this phenomenon as "*macroscopic* $1/f$ behavior" in order to contrast it with the well-known $1/f$-*power* spectrum of the continuous-time stochastic Brownian motion signal (with a continuous single-branch spectrum).

The sequence $\boldsymbol{f}_{n+1}$ is obtained from $\boldsymbol{f}_n$ by concatenating M properly translated copies of $\boldsymbol{f}_n$. This makes $\boldsymbol{f}_n$ somehow contained in $\boldsymbol{f}_{n+1}$, and the resulting self-similarity is also present in the corresponding DFT sequences, albeit in another form. Indeed, $|\boldsymbol{F}_{n+1}|$ can be obtained from $|\boldsymbol{F}_n|$ by first inflating the $|\boldsymbol{F}_n|$ pattern (see, e.g., Figs. 3 and 4) in "frequency" by a factor M (as $F_{n+1}(pM) = F_n(p)$, see (21)). Then new "frequency" points, which are the nonmultiples of M, are added. These points have their amplitudes distributed over a new group of branches which is similar to the groups of branches which are already present in $|\boldsymbol{F}_n|$, but with a magnitude M times lower than the lowest group of branches displayed in $|\boldsymbol{F}_n|$ (downshift over an actual distance $\log M$ on the logarithmic amplitude scale). Observe that the maximal amplitude level does not change as n increases (except for the average signal value $F_n(0) = nF_1(0)$, which may grow without bounds when $F_1(0) \neq 0$, but this does not affect the rest of the spectrum). It is not difficult to imagine that in the actual limit $n = \infty$, one would find an infinite number of groups of "perfect" $1/f$ branches. Each group, except the leftmost one, lies at a distance M times further than its left-neighboring group . The first element in each group has amplitude

$$\lim_{n\to\infty} |F_{n,n}(1)| = \frac{M}{\pi} \sin\left(\frac{\pi}{M}\right) |F_1(1)|$$

(see (30)).

Looking at the spectral pattern on a log-log scale (see, e.g., Fig. 5), going from $|\boldsymbol{F}_n|$ to $|\boldsymbol{F}_{n+1}|$ would first shift the $|\boldsymbol{F}_n|$ pattern to the right over a distance $\log M$, while a new group of branches (called "band" for obvious reasons) appears to the left. The "straight" $(1/f)$ parts of the bands in $|\boldsymbol{F}_{n+1}|$ thereby increase in length by an amount of $\log M$ as compared to the length of the bands in $|\boldsymbol{F}_n|$. The actual limit for $n \to \infty$ produces a pattern in which a first straight $1/f$ band (the straightness would extend to ∞) repeats itself periodically to the right, the period being $\log M$.

Thus far we have not considered any kind of genuine fractal limit signal (with details on infinitely small scales) which could be associated with these sequences. The rigorous treatment of this is a nontrivial matter which raises fundamental questions. An indication of the related problems can be found in [3], where the limit of the point sets $P_n = \{k \mid f_n(k) = \text{given constant}\}$ for $n \to \infty$ have been studied for integer generators. The following gives a hint about the nature of such a limit.

First, we need some form of "continuous-time" signal to be associated with the discrete sequences $\boldsymbol{f}_n$, such as the piecewise-constant function $U_n(t) = f_n(\lfloor t \rfloor)$ for $t \in [0, M^n)$, while $U_n(t) = 0$ for $t \notin [0, M^n)$. It is well known (see, e.g., [6]) that the DFT $\boldsymbol{F}_n$, as defined in (14), is an approximation of the ("continuous") Fourier transform $\mathcal{F}_n(\nu)$ of $U_n(t)$: for $l = 0, 1, \ldots \lfloor M^n/2 \rfloor$: $F_n(l) \approx (1/M^n)\mathcal{F}(l/M^n)$ (the argument of $\mathcal{F}$ expressed in hertz). Note that nothing has been said about the Fourier spectrum for

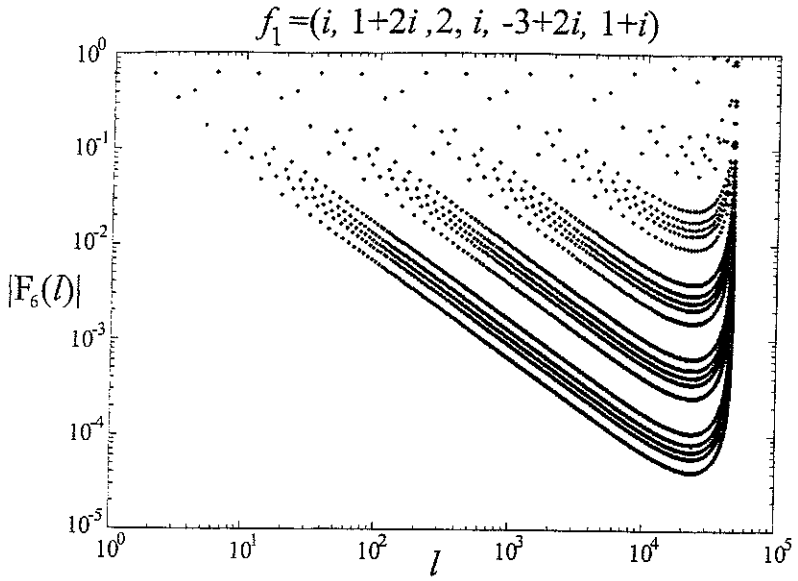


Fig. 5. The log-log graph of the amplitude spectrum $(F_6(l))_{l=1,\ldots,5^6-1}$ of the signal $\boldsymbol{f}_6$ obtained from the complex generator $\boldsymbol{f}_1 = [i,\ 1+2i,\ 2,\ i,\ -3+2i,\ 1+i]$ $(M=6)$. It illustrates the "macroscopic $1/f$-behavior" for $l \ll M^n = 5^6$. As $\boldsymbol{f}_1$ is complex, there are $n=6$ groups of $M-1=5$ branches.

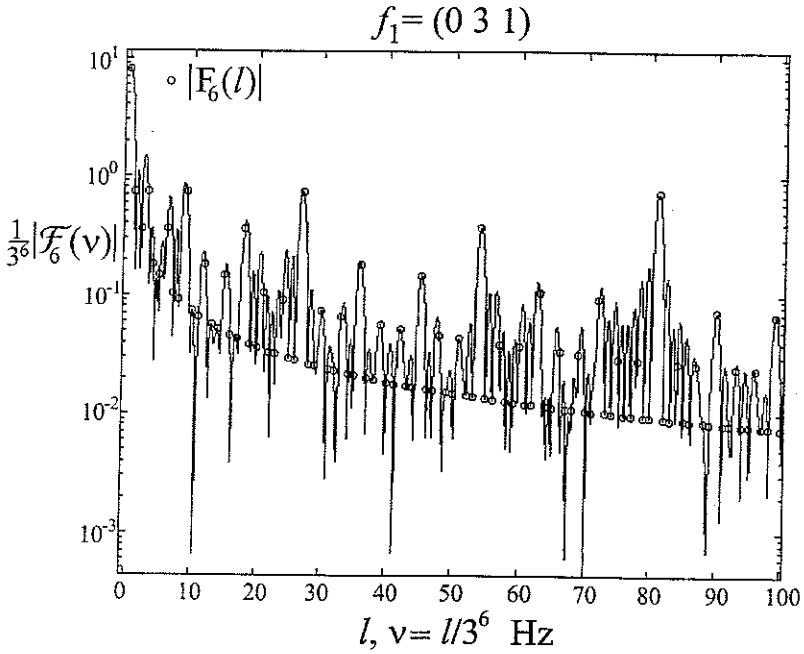


Fig. 6. Comparing the DFT $\boldsymbol{F}_6$ (o) of the sequence $\boldsymbol{f}_6$ obtained from the generator $\boldsymbol{f}_1 = (031)$ and the Fourier transform $\mathcal{F}_6$ of the corresponding piecewise-constant signal $U_6(t)$.

$\nu \neq l/M^n$. Fig. 6 compares, for $\boldsymbol{f}_1 = (031)$ the DFT $\boldsymbol{F}_6$ and the Fourier transform $\mathcal{F}_6$ of the corresponding piecewise-constant signal $U_6(t)$ (approximated by the DFT of the sequence $\boldsymbol{f}_6$ of length $3^6 = 729$) concatenated with a sequence of 8×729 zeros in order to increase the resolution).

In order to construct a genuine fractal limit, $U_n(t)$ should be properly rescaled in amplitude and time. For example, let us consider the signal

$$\hat{U}_n(t) = \frac{1}{n} U_n\left(\frac{n}{M^N} t\right).$$

The amplitude rescaling by the factor $\frac{1}{n}$ makes that the maximal and minimal values in $\hat{U}_n$ are independent of n, and thus equal the maximum $f_{1,\max}$ and minimum $f_{1,\min}$ of the generator $\boldsymbol{f}_1$, respectively. The time rescaling of U_n by the factor $\frac{n}{M^N}$ squeezes the resulting signal $\hat{U}_n$ in the interval $[0,\ n)$. The time extent of $\hat{U}_n$ thus grows with n. The whole rescaling makes the average of the signals $\hat{U}_n$ constant. Denoting the Fourier transform of $\hat{U}_n(t)$ by $\hat{\mathcal{F}}_n(\nu)$, the relationship with the DFT $\boldsymbol{F}_n$ becomes

$$F_n(l) \approx \hat{\mathcal{F}}_n\left(\frac{l}{n}\right), \qquad \text{for } l = 0,\ 1,\ \ldots,\ \lfloor M^n/2 \rfloor$$

an approximation which becomes better as the sampling distance $\frac{n}{M^n}$ in the time domain becomes smaller, i.e., as n increases. As long as $n \in \mathbb{N}$, i.e., n is finite, there is no problem with the nature of the signal $\hat{U}_n(t)$ or its Fourier transform. The very limit $\hat{U}_\infty$, however, is no longer a "normal" signal: its graphical representation for $t \geq 0$ has a "plane-filling" character that fills the horizontal strip between the

values $f_{1,\max}$ and $f_{1,\min}$ (in the limit, one finds at any $t \geq 0$ something similar to what is dispayed in Fig. 1, but infinitely squeezed in time). In view of this, it is also no surprise that the corresponding limit $\hat{\mathcal{F}}_\infty$ of the Fourier transform of $\hat{U}$ is also not something regular. The closest image we can think of, on a log-log scale representation for the amplitude spectrum of the corresponding DFT, is the one that shifts the (limiting) periodic straight-band pattern discussed above over a distance $\log\ n|_{n=\infty}$ to the left (corresponds to the frequency scaling $1/n$). But this distance is rather undefined. Moreover, the actual "continuous" Fourier spectrum interpolates the discrete spectrum in a certain way.

We conclude that considering a genuine fractal limit is not trivial, if it makes sense at all. However, as long as the finite signals $\boldsymbol{f}_n$, U_n, their DFT or ordinary Fourier transform and possible finite rescaling thereof are considered, no interpretation problems arise.

REFERENCES

[1] A. Barbé, "On a class of fractal matrices (I): Excess-matrices and their self-similar properties," *Int. J. Bifurcation and Chaos*, vol. 2, no. 4, pp. 841–860, Dec. 1992.

[2] ——, "On a class of fractal matrices: II. Distribution and scale dependent fractal dimensions of integer sets in excess-matrices and their disguises," *Int. J. Bifurcation and Chaos*, vol. 3, no. 5, pp. 1195–1223, Oct. 1993.

[3] ——, "On a class of fractal matrices:III. limit structures and hierarchical iterated function systems," *Int. J. Bifurcation and Chaos*, vol. 5, no. 4, pp. 1119–1156, Aug. 1995.

[4] M. F. Barnsley, *Fractals Everywhere*. New York: Academic, 1988.

[5] J. M. Blackledge, "On the synthesis and processing of fractal signals and images," in *Applications of Fractals and Chaos*, A. J. Crilly, A. J. Earnshaw, and H. Jones, Eds. Berlin, Germany: Springer-Verlag, 1993, pp. 81–99.

[6] W. L. Brigg and V. E. Henson, *The DFT: An Owner's Manual for the Discrete Fourier Transform*. Philadelphia, PA: SIAM, 1995.

[7] J. Feder, *Fractals*. New York: Plenum, 1988.

[8] B. B. Mandelbrot and J. W. Van Ness, "Fractional Brownian motions, fractional noises and applications," *SIAM Rev.*, vol. 10, pp. 422–437, 1968.

[9] H.-O. Peitgen, H. Jürgens, and D. Saupe, *Chaos and Fractals: New Frontiers of Science*. New York: Springer-Verlag, 1992.

[10] G. W. Wornell and A. V. Oppenheim, "Wavelet-based representations for a class of self-similar signals with application to fractal modulation," *IEEE Trans. Inform. Theory*, vol. 38, pp. 785–880, Mar. 1992.

[11] G. W. Wornell, *Signal Processing with Fractals: A Wavelet-Based Approach*. Upper Saddle River, NJ: Prentice-Hall PTR, 1996.